

## Voltage-Activated Ionic Channels and Conductances in Embryonic Chick Osteoblast Cultures

D.L. Ypey<sup>†</sup>, J.H. Ravesloot<sup>†‡</sup>, H.P. Buisman<sup>†</sup> and P.J. Nijweide<sup>‡</sup>

<sup>†</sup>Department of Physiology and Physiological Physics, 2333 AL Leiden, and <sup>‡</sup>Department of Cell Biology and Histology, 2333 AA Leiden, The Netherlands

**Summary.** Patch-clamp measurements were made on osteoblast-like cells isolated from embryonic chick calvaria. Cell-attached-patch measurements revealed two types of high conductance (100–250 pS) channels, which rapidly activated upon 50–100 mV depolarization. One type showed sustained and the other transient activation over a 10-sec period of depolarization. The single-channel conductances of these channel types were about 100 or 250 pS, depending on whether the pipettes were filled with a low K<sup>+</sup> (3 mM) or high K<sup>+</sup> (143 mM) saline, respectively. The different reversal potentials under these conditions were consistent with at least K<sup>+</sup> conduction. Whole-cell measurements revealed the existence of two types of outward rectifying conductances. The first type conducts K<sup>+</sup> ions and activates within 20–200 msec (depending on the stimulus) upon depolarizing voltage steps from <–60 mV to >–30 mV. It inactivates almost completely with a time constant of 2–3 sec. Recovery from inactivation is biphasic with an initial rapid phase (1–2 sec) followed by a slow phase (>20 sec). The second whole-cell conductance activates at positive membrane potentials of >+50 mV. It also rapidly turns on upon depolarizing voltage steps. Activation may partly disappear at the higher voltages. Its single channels of 140 pS conductance were identified in the whole cell and did conduct K<sup>+</sup> ions but were not highly Cl<sup>–</sup> or Na<sup>+</sup> selective. The results show that osteoblasts may express various types of voltage controlled ionic channels. We predict a role for such channels in mineral metabolism of bone tissue and its control by osteoblasts.

**Key Words** ionic channel · membrane conductance · osteoblast · patch-clamp · voltage activated · outward rectification

### Introduction

Transmembrane ionic channels play important regulatory roles in a diversity of cells. In nerve and muscle cells they control excitability or are involved in chemical signal transmission (Hille, 1984). In epithelial cells they allow mass transport or secretion of ions (Peterson & Maruyama, 1984). In endocrine systems they may constitute part of the hormone secretion (Ashcroft, Harrison & Ashcroft, 1984) or hormone effect mechanism (Maruyama et al., 1983). In the immune system they may be involved in T lymphocyte stimulation (DeCoursey et

al., 1984) and cellular immunity by macrophages (Nelson et al., 1985).

Recently interest has been shown in the role of transmembrane potentials and ionic currents in the function of cells involved in bone tissue metabolism (Dixon, Aubin & Dainty, 1984; Ferrier & Ward, 1986; Edelman, Fritsch & Balsan, 1986; Ferrier et al., 1987; Ypey et al., 1987). Examples of such bone cells are osteoblasts or bone forming cells, osteocytes, which are osteoblasts encapsulated in the mineral bone structure and osteoclasts, which are bone resorbing cells. All three cell types are under endocrine control. Osteoblasts and osteoclasts, for example, have receptors for parathyroid hormone (PTH) and calcitonin (CT), respectively (Nijweide, Burger & Feyen, 1986). Since these cells mediate mass ion transport, e.g., of Ca<sup>2+</sup> ions, between the blood and the bone compartment, ionic channels may be expected to play a role in this transport. In addition, ionic channels may be involved in endocrine signal transmission to bone cells (Edelman et al., 1986; Ferrier et al., 1986), leading to activation or suppression of specific cell functions. Therefore, we have looked for ionic channels in osteoblast-like cells from primary cultures. In particular, we have asked the question whether these cells have voltage-activated channels, as membrane potential control of transmembrane conduction of ions may be an essential aspect of the regulation of transcellular mass transport of ions or of transmembrane signaling.

Here we report that cells from embryonic chick osteoblast cultures do have various types of voltage-activated channels and conductances. So far, we have mainly found depolarization activated channels, sometimes with complex kinetics. These findings reveal membrane biophysical aspects of bone tissue physiology, the importance of which has not been fully recognized as yet. The results provide a basis for future investigations into the role

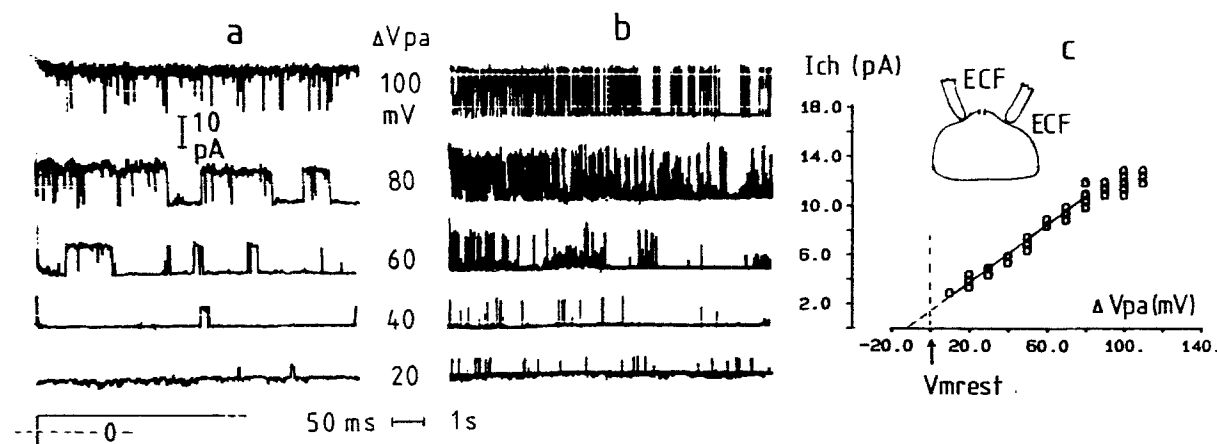


**Fig. 1.** A 117-pS depolarization-activated channel measured in a cell-attached patch with an ECF-filled pipette (OB cell from 1-day culture). The seal resistance was 100 GΩ. (a) Single-channel activity upon depolarizing voltage steps from hyperpolarized patch membrane potentials (see protocol in Materials and Methods). The records of the outward channel currents show how rapidly the channel responds (within 50 msec at the higher depolarizations). The mean open time increases with depolarization. (b) The same records as in a but on a slower time scale, showing sustained activity during the 10-sec depolarizations. (c) Linear single channel *I-V* curve with a slope of 116.9 pS and a reversal potential at 12.3 mV hyperpolarization (67 data points, partly superimposed, 43 of which were used for curve fitting in the linear range, where the *I-V* curve does not saturate). *Ich* = single channel current,  $\Delta V_{pa}$  = applied change in patch potential,  $V_{mrest}$  = resting membrane potential of the cell

of voltage controlled ionic channels in mineral metabolism of bone tissue, including  $\text{Ca}^{2+}$  transport between the blood and bone tissue and its endocrine control.

## Materials and Methods

Osteoblast-like cells (OB's) were isolated from 18-day old embryonic chick calvaria and were cultured for 1–11 days (Nijweide, van der Plas & Scherft, 1981). Membrane currents were measured at room temperature (21–24°C) in the cell-attached-patch and the whole-cell configuration of the patch-clamp technique (Hamill et al., 1981) with the use of a L/M EPC5 amplifier (List Electronic, Darmstadt/Eberstadt, West Germany). In some of the cultures, the cells were patched using high resolution microscopy with a 100× oil immersion objective (Ince, van Dissel & Diesselhoff, 1985). This made it easier to recognize cell morphology and to obtain stable seals on flat, adhered cells.

The cells were bathed in a standard extracellular salt solution (Extracellular Fluid, ECF) with composition (in mM): 150 NaCl, 3 KCl, 1  $\text{MgCl}_2$ , 4  $\text{CaCl}_2$  and 10 HEPES/NaOH (pH 7.2). In some cell-attached-patch experiments the patch pipette was filled with the same extracellular solution. In other cases the pipette contained the intracellular solution (Intracellular Fluid, ICF) used for whole-cell recording composed of (mM): 0 NaCl, 143 KCl, 2  $\text{MgCl}_2$ , 1  $\text{CaCl}_2$ , 11 EGTA and 10 HEPES/KOH (pH 7.2), unless mentioned otherwise. These ECF and ICF were chosen to be able to detect  $\text{K}^+$  channels and conductances (cf. Ypey & Clapham, 1984).

"Giga-seals" (cf. Hamill et al., 1981) were obtained from about half of the 160 cells, selected from 26 cultures over a period of two years. In about 25% of the cell-attached patches obtained the conditions were favorable enough to allow the iden-

tification of various types of voltage-dependent single channels. In total, 15 whole cells were obtained.

Voltage dependency of cell-attached-patch channels was tested by applying a standard stimulus protocol of subsequent pulses of 10-sec duration starting from zero pipette potential. The sequence was 0, -10, +10, -20, +20, -30, +30, mV, . . . etc. Outward current is plotted upward in all figures.

Series resistances in the whole-cell experiments were 10–100 MΩ, thus reducing the measured whole-cell current at high membrane conductances (>1 nS) in some cases.

Signals were filtered with 24 dB per octave low pass filters at a cut-off frequency of 1 kHz, unless mentioned otherwise.

Single-channel conductances and reversal potentials when given as means  $\pm$  SD for a given *n* were obtained from least squares fits of a linear curve to *n* data points of a current-voltage (*I-V*) plot. Other values were obtained from fits by eye.

## Results

### CELL-ATTACHED-PATCH RECORDINGS

#### *Channels Facing an Extracellular Low $\text{K}^+$ Saline*

The cell-attached-patch recordings with pipettes filled with the standard extracellular salt solution (ECF, a NaCl Ringer with 3 mM  $\text{K}^+$ ) allowed us to observe the activity of single transmembrane channels facing the normal, intracellular cytoplasmic fluid at one side and a more or less normal extracellular fluid at the other side. Cells from six cultures were patched with ECF-filled pipettes. Cell-attached patches of six cells showed consistent re-

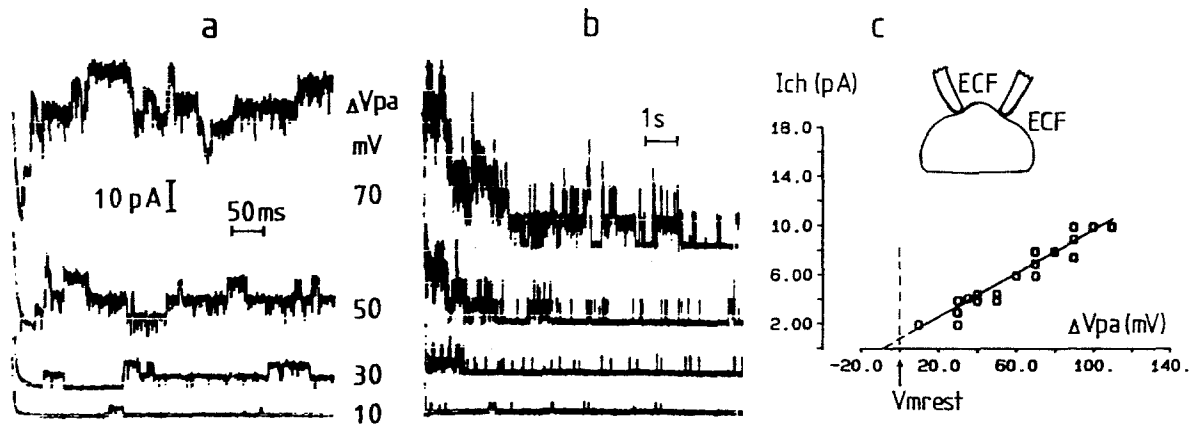


**Fig. 2.** An 87-pS depolarization-activated channel with transient activation. Cell-attached-patch records were made with ECF-filled pipettes (OB-cell from 1-day culture). (a) Records of the outward channel currents at a fast time scale to show rapid channel opening at the larger depolarizing steps. The 70-mV depolarization records show at least 7 channels in the patch. (b) The same records as in a but on a slower time base, revealing the transient nature of activation. (c) Linear single channel  $I$ - $V$  curve with a channel conductance of 86.6 pS and a reversal potential of 9.1 mV below the resting membrane potential of the cell (83 data points)

producible voltage and time-dependent single-channel activity during the seal. One type of channel activity is illustrated in Fig. 1. The cell measured was a flat cell in contact to a few other cells (1 day culture). The records are from a patch probably containing only one channel of the type and size illustrated, since double channel openings were not observed during the whole 15-min experiment (*cf.* Fig. 1a,b). Occasional channel openings can be seen at 20 mV depolarization as outward current steps. Channel opening is activated by depolarizing (i.e., negative pipette) potentials (Fig. 1a,b). The channel currents are rectangular in shape, indicating ideal voltage clamp conditions, i.e.,  $R_m \ll R_{ch}$  with  $R_m$  for membrane resistance of the attached cell and  $R_{ch}$  for the resistance of the channel in the patch (*cf.* Hamill et al., 1981). Channel openings occur more frequently at 60 mV depolarization, while the channel is mainly in the open state at 100 mV depolarization.

Channel opening occurs with shorter (first) latency times upon larger depolarization steps (within milliseconds at steps of 70 to 110 mV, *cf.* Fig. 1a). Upon repolarizing steps back to the resting or a hyperpolarized condition channel closing (deactivation) occurs rapidly as well (within 50 msec, *data not shown*). During depolarizations maintained for 10 sec, channel activity is sustained, though there may be some decline (Fig. 1b). The channel current grows with depolarization and has a reversal potential of  $12.3 \pm 1.8$  mV (SD,  $n = 43$ ) more negative than the resting membrane potential of the cell (Fig. 1c). Reversed channel currents were not observed at hyperpolarizing pipette potentials ( $V_{pip}$ ). The single-channel current-voltage ( $I$ - $V$ ) curve, which is

linear for depolarizations up until 80 mV, yields a single-channel conductance of  $116.9 \pm 3.2$  pS (SD,  $n = 43$ ).

The same type of channel was found in cell-attached patches of two other cells, one of the same 1-day culture and one of a 2-day culture. In these cells sustained activity was even a more striking property. The other patch of the 1-day culture contained a few channels ( $>4$ ). In this case time and voltage-dependent behavior upon depolarizing voltage steps was reflected rather in the mean number of open channels instead of in the mean open time of a single channel. In this cell the recording conditions were not ideal. The channel currents were not rectangular but showed an exponential decay, indicating that  $R_m$  was in the order of  $R_{ch}$ , thus limiting the current through the open channel (Nelson et al., 1985). Allowing for this property, the single-channel conductance was estimated to be 91 pS and the reversal potential 14 mV below the resting membrane potential. The patch from the 2-day cell contained a 90-pS channel with a reversal potential 30 mV below the resting membrane potential.

A second type of channel was identified in cell-attached patches from three 1-day cells. Measured with ECF-filled pipettes, this channel had a similar voltage and time-dependent activation (Fig. 2a) with a similar  $I$ - $V$  curve (Fig. 2c). Its slope was  $86.6 \pm 2.9$  pS (SD,  $n = 83$ ) and it reversed at  $9.1 \pm 3.1$  mV (SD,  $n = 83$ ) hyperpolarization. However, the channel differed markedly from the first type in having only transient activation. The rapid phase of activity increase is followed by a slow decrease to almost zero activity with a time constant of a couple of seconds (Fig. 2b). The channel activity illustrated

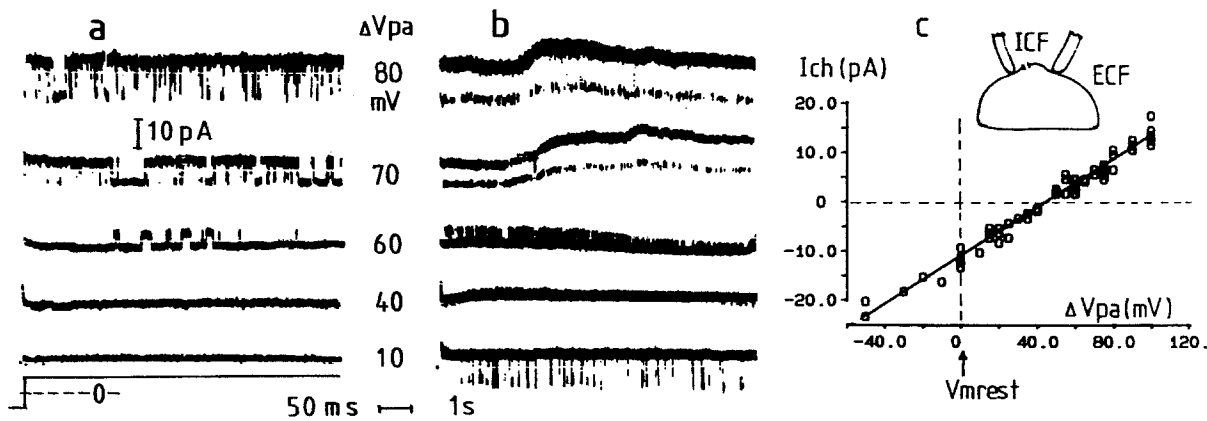


**Fig. 3.** A 247-pS depolarization-activated channel measured in a cell-attached patch with an ICF-filled pipette (OB cell from 3-day culture). The ICF contained 1 mM EGTA. (a) Records at a 50-msec time base, showing the effect of depolarization on the mean open time of the channel. Channel opening is rapid upon the higher depolarizing steps. (b) The same records on a 1-sec time base, showing sustained channel activity during maintained depolarization. Note the slow fluctuations in background current, probably representing changes in the membrane potential of the attached cell, since these changes are associated with fluctuations in the single-channel current amplitude. (c) Linear *I-V* curve of the channel with a slope of 247.0 pS and with current polarity reversal at 43.7 mV depolarization (73 data points)

is from a patch having about seven 87-pS channels. Apparently no other channels of this or larger size were present. The time course of the increase and decrease of activation is visible as a change in the mean number of open channels, with each channel maintaining a constant current amplitude. The channels of the other two patches had conductances of 87 and 90 pS and reversal potentials of 23 and 25 mV hyperpolarization of the resting membrane potential, respectively.

#### *Channels Facing an Extracellular KCl Ringer*

In order to further characterize the cell-attached-patch channel activity found in ECF we studied the effect of high extracellular  $K^+$ . The pipettes were filled with the intracellular solution (ICF, with 143 mM  $K^+$ ) and the same sequences of voltage steps (see Materials and Methods) were applied as in the ECF experiments.

The cell-attached patches obtained were often those preceding whole-cell measurements (see below). We found various types of channels, mainly depolarization activated channels. Channels with high rates as well as low rates of opening and closing were observed. In two cases we could identify channels as being hyperpolarization activated. Occasionally, channel activity at resting conditions was not potential dependent or only weakly so.

In particular, we describe two types of large size depolarization-activated channels, corresponding to the two types of channels described above for ECF-filled pipettes. The first is again a sustained-activity type as illustrated in Fig. 3 for a 3-day cell. The channel only occasionally opens at the resting

membrane potential but opens much more frequently around its reversal potential, which is  $43.7 \pm 0.7$  mV (SD,  $n = 73$ ) more positive than the resting potential (Fig. 3c). Activation turns on rapidly (within 50 msec) at large depolarization steps (70 mV) but no significant decrease in activation is visible during depolarizations sustained for 10 sec (Fig. 3b). The single-channel conductance is as large as  $247.0 \pm 4.7$  pS (SD,  $n = 73$ ), at least twice as large as that of the sustained-activity channel in ECF.

The same type of channel was found in two 1-day cells (one is illustrated in Fig. 7) and in one 3-day cell. These cells had channels with conductances of 230–250 pS and reversal potentials at 30–35 mV depolarization of the resting membrane.

The second type of channel has a peak-shape transient in activation (Fig. 4, 1-day culture). It activates rapidly in the same range of depolarization as the first channel type in ICF and also shows a subsequent slow but significant decline in activity. Channel current reverses polarity at  $36.2 \pm 0.5$  mV (SD,  $n = 87$ ) depolarization. The single-channel conductance is  $162.2 \pm 2.7$  pS (SD,  $n = 87$ ), again considerably larger than that of the second channel type in ECF. No channels of 100–250 pS conductance were found in extracellular ICF, reversing at hyperpolarized membrane potentials, as in ECF.

#### WHOLE-CELL CONDUCTANCES

##### *A Transient Outward $K^+$ Current Activated Below 0 mV*

In five whole cells of 5 to 11-day cultures we found an outward rectifying  $K^+$  conductance. The cells, in

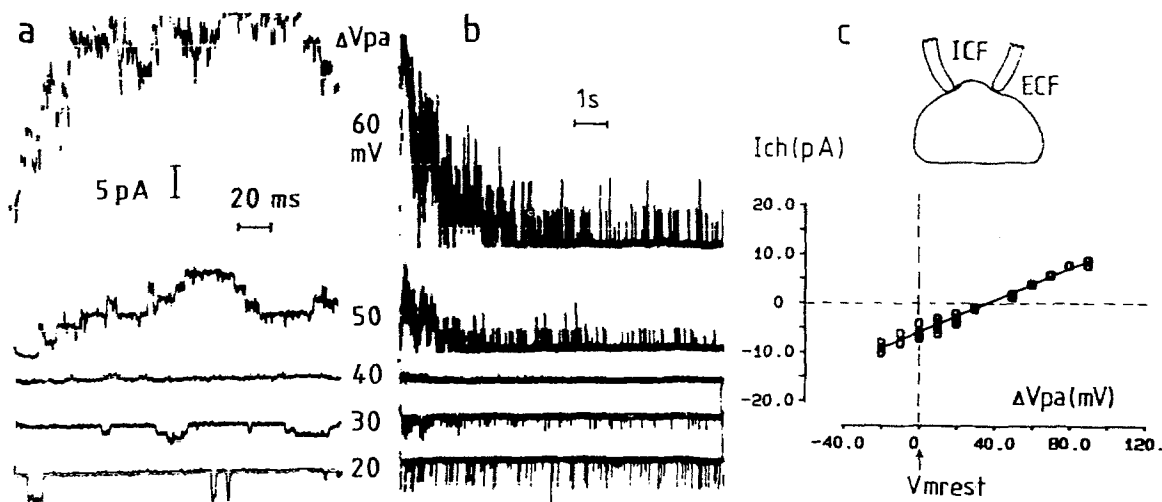


**Fig. 4.** A 162-pS depolarization-activated channel with transient activation. The cell-attached-patch records were made from a rounding 1d-OB cell, with ICF-filled pipettes (ICF with 1 mM EGTA). (a) Records at a 20-msec time base to show the rapid opening of the channels at the higher depolarizing steps and the reversal of the channel currents around 40 mV depolarization. (b) Records at a 1-sec time base to show the decline of activation. (c) Linear  $I$ - $V$  curve of the channel with a slope of 162.2 pS and with current polarity reversal at 36.2 mV depolarization (87 data points)

which this conductance was found, were rounding off for cell division. For our conditions of whole-cell measurements this conductance appeared in isolation from other conductances. It turns out upon steps from holding potentials of between  $-60$  and  $-100$  mV to potentials of  $-30$  mV and higher (cf. Fig. 5a). The rapid phase of activation is followed by a slow phase of inactivation (Fig. 5b). Activation occurs faster at more positive potentials. At  $-20$  mV half-maximal activation occurs within 50 msec. At  $+40$  mV activation is half maximal in about 5 msec (Fig. 5a). Inactivation is not very voltage dependent, if there is any dependency. The time course of inactivation follows a single exponential curve until it is almost complete (Fig. 5b,e). Time constants determined from semilog plots were between 2.1 and 3.6 sec at voltages between 0 to  $+40$  mV (3 whole cells). Deactivation is voltage dependent (Fig. 5c). Upon back-steps to more hyperpolarized potentials during peak activation, deactivation occurs within about 150 msec at  $-20$  mV but within 50 msec at  $-60$  mV. Recovery from inactivation is a two-phase process (Fig. 5d). The initial rapid phase occurs within 2 sec, but the slow phase takes at least 20 sec. The back-step experiment used to study deactivation also showed that this conductance, given the composition of the extra- and intracellular solution used, primarily conducts  $K^+$  ions. The deactivating current tails reverse at (Fig. 5c) or somewhat below  $-80$  mV ( $-85$  mV, other cells), close to the calculated  $K^+$  Nernst potential  $E_K = -97$  mV but far from the  $Cl^-$  Nernst potential,  $E_{Cl} = 0$  mV, and from the positive, undefined  $Na^+$  Nernst potential,  $E_{Na}$ . Using  $E_K$  for the

reversal potential and assuming a linear behavior of the conductance, maximal conductance varied between at least 1.8 and 4 nS for the different cells (cf. Fig. 5e).

The semi-stationary  $I$ - $V$  curve (Fig. 5e) crosses the  $V_m$ -axis around  $-27$  mV. This was also the approximate value of the resting membrane potential in current-clamp conditions, where it fluctuated between  $-25$  and  $-35$  mV. The membrane resistance at that potential was at least  $4 G\Omega$ .

For our whole-cell conditions no indications were found of other voltage controlled conductances in the voltage range of  $-160$  to  $+20$  mV (Fig. 5c), i.e., no hyperpolarization activated  $K^+$  conductances nor depolarization activated inward currents. This was surprising, since cell-attached patch records, in one case even from the same cell in which this outward rectifier was found, suggested the existence of hyperpolarization-activated channels.

Single-channel activity may be expected in the tails of the inactivating currents of Fig. 5b, if inactivation does not affect the single-channel conductance but involves a decline of the probability of the channels being open, as is the case in macrophages (Ypey & Clapham, 1984). Given the resolution of the records and assuming one open channel state, we conclude that the channels of this whole-cell conductance have a conductance smaller than 30 pS.

The outward rectifying conductance illustrated in Fig. 5 was not found in any of the other 10 whole cells in younger cultures (1–3 days), except probably in one case where a similar conductance was

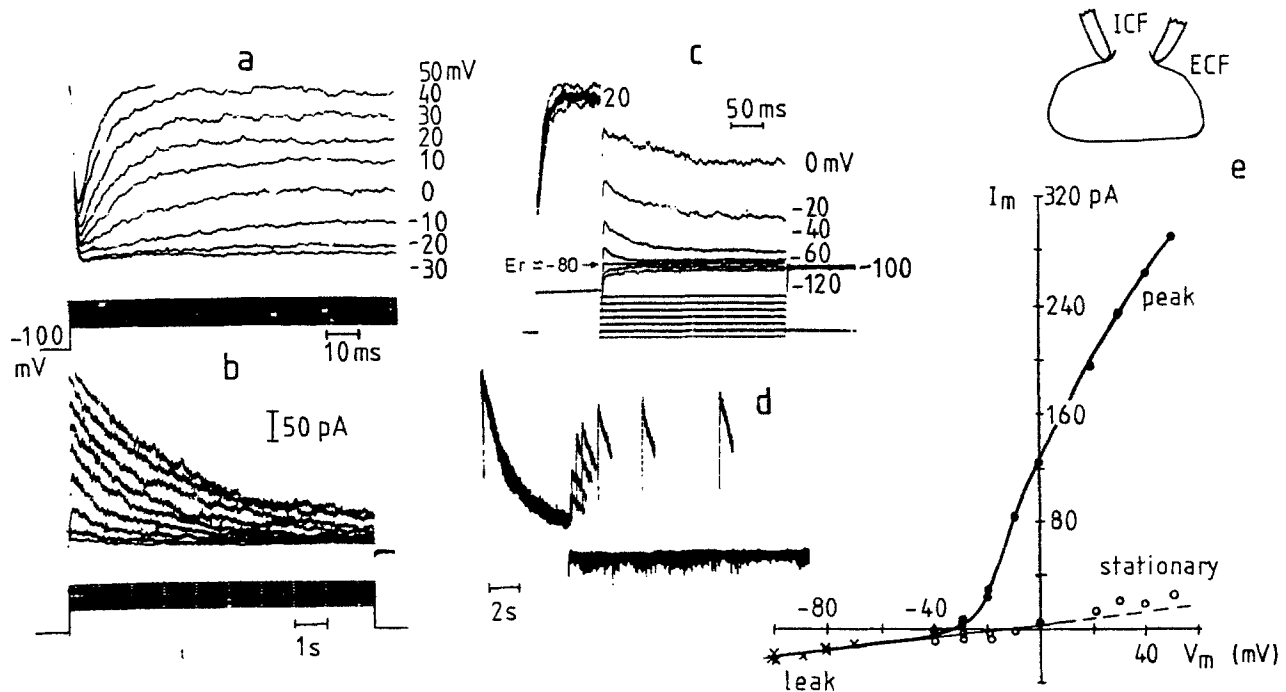


**Fig. 5.** Kinetic properties of the outward-rectifying  $K^+$  conductance of a 6-day OB cell. The cell was spheroid with a  $13.5\text{-}\mu\text{m}$  diameter. The holding potential was  $-100\text{ mV}$ . The current calibration in *b* also applies to *a*, *c*, and *d*. (*a*) Superimposed records of the rapid onset of the current upon depolarizing steps from  $-100\text{ mV}$  to the potentials indicated. (*b*) Superimposed records showing the slow single-exponential inactivation. The current traces are from the same records as in *a*. Pulse duration and resting interval were  $10\text{ sec}$ . The slight deviation from single-exponential decline at  $+30$  and  $+40\text{ mV}$  is probably due to seal noise. (*c*) Superimposed records of deactivation upon hyperpolarizing back-steps during peak activation at  $20\text{ mV}$ . The 2-step pulses were applied at  $10\text{-sec}$  intervals. The current tails reverse at  $E_r = -80\text{ mV}$ . Even at the most negative back-step to  $-160\text{ mV}$  (not shown), no other voltage-activated conductances were present. (*d*) Two-phase recovery from inactivation. Superimposed current traces obtained by applying conditioning  $5\text{-sec}$  duration depolarizing pulses of  $+20\text{ mV}$  followed by a variable recovery period and a  $1\text{-sec}$  test pulse at  $+20\text{ mV}$ . Resting intervals between the pulse pairs were  $24$  to  $76\text{ sec}$ . (*e*) Current-voltage relationship derived from a run like that in *a* and *b*, but earlier in this whole-cell experiment of  $50\text{-min}$  duration. Filled circles represent peak values, open circles give the (almost) stationary currents at the ends of the  $10\text{-sec}$  depolarizing pulses and crosses indicate the size of the background current in the absence of the outward rectifier. Peak values of this plot were slightly under those from the run illustrated in *b*

found, but with slower inactivation. In another case a different type of outward conductance was found, which already activated above  $-60\text{ mV}$  but which showed only partial inactivation.

#### *An Outward Rectifier Activated at Positive Membrane Potentials*

In four 1-day OB-cells we found an outward rectifying conductance, activated at extreme depolarizations under our conditions of whole-cell measurements (very low intracellular calcium concentrations). Figure 6 illustrates its properties. Upon voltage steps from  $0$  to  $+60\text{ mV}$  channel activity appears rapidly with only occasional double channel openings and remains during the  $10\text{-sec}$  depolarization (Fig. 6*a*). At larger depolarizing steps double and multiple channel openings occur much more frequently (up to at least  $10$  levels) and a slow inactivation-like process becomes visible as a partial de-

crease in the mean number of open channels. Obviously this channel is the dominant channel present. At  $80\text{ mV}$  channel activity was stationary after a  $20\text{-sec}$  transient for at least  $2\text{ min}$  at  $70\%$  of the initial mean current. Figure 6*b* illustrates the outward rectifying nature of this conductance in the current voltage ( $I$ - $V$ ) relationship. In this case the peak values of the mean currents just after the steps in voltage were plotted. For the four cells measured these peak currents ranged from  $60$ – $340\text{ pA}$  at  $100\text{ mV}$ . The degree of 'inactivation' and the voltage range of activation also showed some variability.

The  $I$ - $V$  curve of the single channel could be measured in two whole cells and one of those is illustrated in Fig. 6*c*. It is linear with a single-channel conductance of  $144.4 \pm 0.5$  (SD,  $n = 57$ ) pS below  $+80\text{ mV}$ , but saturates above  $+80\text{ mV}$ , i.e., in the voltage range where the channels are strongly activated. The reversal potential  $E_r$  of the channel, estimated by extrapolation, is  $-36.3 \pm 2.6$  (SD,  $n = 57$ ) mV. The channels activate and deactivate

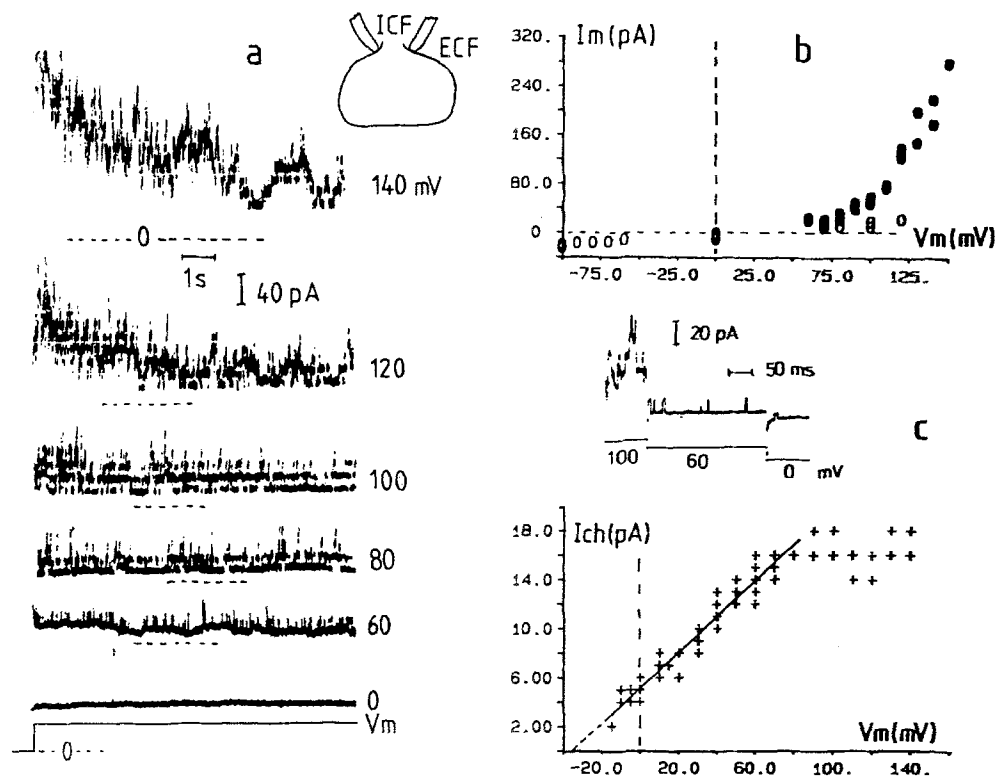


**Fig. 6.** Properties of the large-depolarization activated outward rectifier of a 1-day OB cell, measured in the whole-cell configuration. (a) Current responses to step depolarizations from 0 mV to the various values indicated. The increase in current with depolarization and its subsequent decrease at the higher potentials results from changes in the mean number of open channels, while the single-channel amplitude remains constant. Zero-current baselines are indicated by dashed lines. (b) Initial mean peak values upon step depolarizations as in a. Repeated values are given because of the large variability. Open symbols represent leak currents. Leak values in the range of voltage where the channels activate are current values while no channels were open. (c) Single-channel  $I-V$  curve from the whole cell of a (79 data points). The inset illustrates this  $I-V$  with channel currents at 3 potentials. At the same time it shows that channel opening rapidly changes with the applied potential (within a few msec). The straight line is fitted to the 57 data points below 90 mV

within a few msec (see inset Fig. 6c). This made it impossible to see channel currents below the reversal potential and to determine  $E_r$  precisely, but the estimated value of  $E_r = -36$  mV indicates that the channel at least conducts  $K^+$  ions, though not very selectively, as the  $K^+$  concentration gradient for the solutions used is the only one providing a negative  $E_r$  of  $E_K = -97$  mV.

In two of the OB cells with this outward conductance the whole-cell configuration was preceded by a cell-attached patch with the 250 pS sustained-activity type of channel described above. Figure 7 illustrates the similarity between the voltage-dependent behavior of the single channel and that of the whole-cell conductance during voltage ramps instead of steps. The channel, as well as the conductance, is depolarization activated. The ramp responses looked, on the average, symmetrical, consistent with the sustained activity observed for the same channel and conductance during long-duration depolarizing voltage steps. The channel current reverses at 35 mV depolarization of the mem-

brane patch, but significant activation requires at least 70 mV depolarization. Thus, this channel may be the one constituting the whole-cell conductance, when the cell is intact.

## Discussion

The present paper gives a description and patch-clamp analysis of voltage controlled ionic channels and conductances in a primary osteoblast culture. The channels and conductances described are depolarization activated with rapid activation and deactivation, i.e., occurring within 5–50 msec.

Generally speaking, the cell-attached-patch results showed the existence of at least two types of depolarization-activated high conductance channels, one having sustained activation and the other having transient activation. However, both types had different channel conductances and reversal potentials, depending on the pipette solution used.

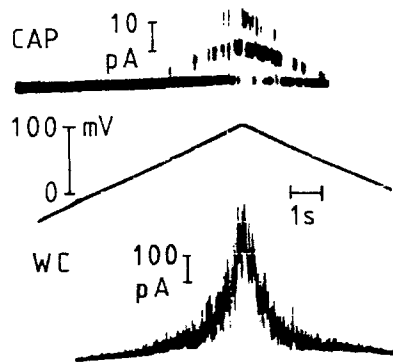


Fig. 7. Similarity between the voltage-gated behavior of a cell-attached patch (CAP) channel (upper record) and that of the whole-cell conductance (WC, lower record) activated at extreme depolarization in the same cell (no simultaneous records). The voltage ramp (middle record) illustrated is the applied membrane potential for the whole cell, but it also represents the change in patch potential (from the unknown resting membrane potential) for the cell-attached patch. Pipette was filled with ICF

The direction of the changes in channel conductance and reversal potential were consistent with at least  $K^+$  conduction through the channels. In high external  $K^+$  (143 mM) the channel conductance was increased, as may be expected from an effect of ionic strength on channel conductance (Hille, 1984). In addition, the reversal potential was then 30–45 mV more positive than the resting potential instead of 10–20 mV more negative, as in 3 mM external  $K^+$ . Therefore, the two types of channels found with ECF pipettes may be the same channels as those found with ICF pipettes, both conducting at least  $K^+$  ions.

So far we have not noticed substates in the records of the channels described. It is feasible that these substates were masked by variations in channel current amplitudes due to membrane potential fluctuations of the attached cell or to background activity of smaller unresolved channels.

The nature and function of both channel types is yet unclear. A quantitative analysis is required to decide whether the transient channel activity is only a variable quantitative difference between the channel types. Apparently, during maintained depolarization the transiently activated channels enter an inactive state other than the resting closed state. The records (Figs. 2b and 4b) suggest that this inactive state is not an absorbing state, since some channel activity remains, depending on the depolarization. Obviously a sustained-activity channel, if activated in the range of resting potential, would contribute to the resting membrane potential in osteoblasts, while the transient channels may be ex-

pected to play a role in transmembrane signalling or in transient ion transport.

The outward-rectifying  $K^+$  conductance seemed to develop in culture, since it was only found in the older osteoblast cultures (5–11 days). In this and other respects it resembles the  $K^+$  conductance found in peritoneal macrophages (Ypey & Clapham, 1984). However, it activates and inactivates more slowly and its recovery from inactivation is biphasic, i.e., it has an initial rapid phase, which is absent in macrophages. In addition a sigmoidal onset of the currents upon depolarizing voltage steps, as found in macrophages, was not clear from the records. Hence, based on these observations we hypothesize a state diagram for the channels of this conductance with at least one closed state, one open state and two inactivated states.

The reversal potential of this current clearly indicates that this conductance conducts  $K^+$  ions under our experimental whole-cell conditions. However, the deviation from the expected value (–80 instead of –97 mV), suggests that other ions may also permeate through these channels to a certain extent.

The depolarization-activated and transient high conductance channel found in the cell-attached-patch recordings does not underlie the outward-rectifying whole-cell  $K^+$  conductance, since channels of that size would have been observed in the inactivating tails of the whole-cell currents. Thus, the single channels of this  $K^+$  conductance still have to be resolved.

Transient outward  $K^+$  currents of the type found in the present study (Fig. 5) play a significant role in action potential repolarization and repetitive firing in excitable cells such as heart cells (Giles & Van Ginneken, 1985) and nerve cells (Connor & Stevens, 1971). Interestingly, similar outward-rectifying  $K^+$  conductances have been found in various nonexcitable cells such as macrophages (Ypey & Clapham, 1984), T-lymphocytes (DeCoursey et al., 1984), B-lymphocytes (Choquet et al., 1987) and astrocytes (Bevan & Raff, 1985). The function of this outward rectifier in these cells is still unclear.

Because of its extreme inactivation, the outward  $K^+$  conductance in osteoblasts is not suitable for stationary membrane potential or ion transport control. The recent discovery that outward-rectifying  $K^+$  conductances can be controlled by second messengers (Choquet et al., 1987; Grega, Werz & MacDonald, 1987) may be crucial for understanding the role of these conductances in nonexcitable cells.

The outward conductance activated at positive potentials does conduct  $K^+$  ions and is not highly selective for  $Na^+$  and  $Cl^-$  ions. It activates at unphysiological membrane potentials (+50 to +100

mV) under our conditions of whole-cell measurements. We speculate that the voltage range of activation of this conductance may be under control by cytoplasmic factors, as in the calcium-dependent  $K^+$  conductance (Maruyama et al., 1983), which may bring activation into the physiological range of membrane potentials.

The channels underlying this whole-cell conductance had a conductance of 140 pS, which is intermediate between the channel conductances found in the cell-attached-patch for ECF and ICF. Cell-attached patch records preceding whole-cell recordings from the same cell (*cf.* Fig. 7) provided evidence that the sustained-activity 250 pS channels measured in the cell-attached patch with ICF filled pipettes are the channels constituting the whole-cell conductance under consideration. This would imply that the conductance of these channels increases when they face external ICF (with high  $K^+$ ) instead of ECF (with low  $K^+$ ), consistent with  $K^+$  conduction (Hille, 1984). However, this would also imply that the OB cell has a smaller intracellular  $[K^+]$  than ICF, since the sustained channel measured with ECF pipettes in the cell-attached patch (*cf.* Fig. 3) has a conductance of only 90 pS. Taken together, the results of the present study provide reasons to expect that  $K^+$  conduction is important in osteoblast function.  $K^+$  conduction may even serve as a factor controlling transcellular  $Ca^{2+}$  transport through  $Ca^{2+}$  channels, since the rate of transmembrane transport of a given cation may depend on the rate with which another cation can move in the opposite direction through the same membrane in order to maintain electroneutral transport.

The single-channel current records in the cell-attached patch configuration were sometimes exponential instead of rectangular, indicating that the membrane resistance of the attached cell may be in the order of 1–10 G $\Omega$  in intact osteoblasts. Such high cell membrane resistances were also found in whole-cell current clamp measurements, where the membrane potential could be –40 to –60 mV. These results indicate that microelectrode measurements on cultured single osteoblast cells should be interpreted with care, since microelectrode impalement itself may change the membrane potential as well as the condition of the cell by introducing a leakage conductance due to incomplete sealing of the membrane around the electrode tip (Ince et al., 1986).

The cell-attached patch outward channels measured in the present study with ECF-filled pipettes are different from the 55-pS inward channels recently described by Ferrier et al. (1987) for the osteoblast cell line ROS 17/2.8. Their outward 120–150 pS channel, measured with an ICF-like solution,

seems to have a smaller conductance than our outward channel found under comparable conditions (ICF-filled pipettes). In addition, in our whole cells we never found spontaneous periodic current fluctuations in voltage-clamp conditions or voltage fluctuations in current-clamp conditions. Furthermore, our whole-cell membrane resistances were significantly higher than those of Ferrier et al. (1987). This indicates functional differences between the ROS 17/2.8 cell line and cells from primary chicken osteoblast cultures. One difficulty in the present work is the variety in types of channels and conductances to be found in cells selected for patching. During cell-attached-patch experiments the membrane resistance of the attached cell may be as high as that of the channel or much lower. Whole-cell currents may be very different in different cells. This indicates heterogeneity of the cells in the cultures. Periosteal fibroblasts, which are closely related to osteoblasts, may constitute a small percentage of the cells in osteoblast cultures (Nijweide et al., 1981). Cells may be in different stages of the cell cycle or may represent different differentiation stages of the osteoblastic cell line. In this respect it is of interest that the outward rectifying  $K^+$  conductance described in Fig. 5 was found in rounding, dividing cells. This suggests that its presence is related to the stage of the mitotic cell cycle. The latter notion agrees with the suggestion of DeCoursey et al. (1984) that a voltage-gated  $K^+$  conductance very similar to that of the present study (Fig. 5) is involved in the proliferation of T-lymphocytes.

Given the variety in voltage-activated channels found, this study should be seen as a first attempt to categorize the various channels and conductances in osteoblasts with the patch-clamp technique. A further identification of the channels requires a pharmacological and kinetic analysis. The abundant presence of high conductance, voltage-controlled channels is promising for important functional roles of these transport proteins in osteoblasts.

We thank Mr. A. di Bon and Mr. A. van der Plas for preparing the osteoblast cultures. We thank Dr. C. Ince for advice, Mr. K. Jalink for assistance and Dr. M.E. Wise for improvements of the manuscript. This work was supported by the Netherlands Organization for Pure Research (ZWO).

## References

- Ashcroft, F.M., Harrison, D.E., Ashcroft, S.J.H. 1984. Glucose induces closure of single potassium channels in isolated rat pancreatic beta-cells. *Nature (London)* **312**:446–448
- Bevan, S., Raff, M. 1985. Voltage-dependent potassium currents in cultured astrocytes. *Nature (London)* **315**:229–232
- Choquet, D., Sarthou, P., Primi, D., Cazenave, P., Korn, H.

1987. Cyclic AMP-modulated potassium channels in murine B cells and their precursors. *Science* **235**:1211–1214
- Connor, J.A., Stevens, C.F. 1971. Prediction of repetitive firing behaviour from voltage clamp data on an isolated neurone soma. *J. Physiol. (London)* **213**:31–53
- DeCoursey, T.E., Chandy, K.G., Gupta, S., Cahalan, M.D. 1984. Voltage-gated K<sup>+</sup> channels in human T lymphocytes: A role in mitogenesis? *Nature (London)* **307**:465–468
- Dixon, S.J., Aubin, J.E., Dainty, J. 1984. Electrophysiology of a clonal osteoblast-like cell line: Evidence for the existence of a Ca<sup>2+</sup> activated K<sup>+</sup> conductance. *J. Membrane Biol.* **80**:49–58
- Edelman, A., Fritsch, J., Balsan, S. 1986. Short-term effects of PTH on cultured rat osteoblasts: Changes in membrane potential. *Am. J. Physiol.* **251**:C483–C490
- Ferrier, J., Ward, A. 1986. Electrophysiological differences between bone cell clones: Membrane potential responses to parathyroid hormone and correlation with the cAMP response. *J. Cell. Physiol.* **126**:237–242
- Ferrier, J., Ward-Kesthely, A., Homble, F., Ross, R. 1987. Further analysis of spontaneous membrane potential activity and the hyperpolarizing response to parathyroid hormone in osteoblastlike cells. *J. Cell. Physiol.* **130**:344–351
- Giles, W.R., Van Ginneken, A.C.G. 1985. A transient outward current in isolated cells from the crista terminalis of rabbit heart. *J. Physiol. (London)* **368**:243–264
- Grega, D.S., Werz, M.A., MacDonald, R.L. 1987. Forskolin and phorbol esters reduce the same potassium conductance of mouse neurons in culture. *Science* **235**:345–348
- Hamill, O.P., Marty, A., Neher, E., Sakmann, B., Sigworth, F.J. 1981. Improved patch-clamp techniques for high-resolution current recording from cells and cell-free membrane patches. *Pfluegers Arch.* **391**:85–100
- Hille, B. 1984. *Ionic Channels of Excitable Membranes*. Sinauer Associates, Sunderland, Mass.
- Ince, C., Dissel, J.T. van, Diesselhoff, M.M.C. 1985. A Teflon culture dish for high-magnification microscopy and measurements in single cells. *Pfluegers Arch.* **403**:240–244
- Ince, C., VanBavel, E., VanDuijn, B., Donkersloot, K., Coremans, A., Ypey, D.L., Verveen, A.A. 1986. Intracellular microelectrode measurements in small cells evaluated with the patch-clamp technique. *Biophys. J.* **50**:1203–1209
- Maruyama, Y., Petersen, O.H., Flanagan, P., Pearson, G.T. 1983. Quantification of Ca<sup>2+</sup> activated K<sup>+</sup> channels under hormonal control in pig pancreas acinar cells. *Nature (London)* **305**:228–232
- Nelson, D.J., Jacobs, E.R., Tong, J.M., Zeller, J.M., Bone, R.C. 1985. Immunoglobulin-G induced single ionic channels in human alveolar macrophage membranes. *J. Clin. Invest.* **76**:500–507
- Nijweide, P.J., Burger, E.H., Feyen, J.H.M. 1986. Cells of bone: Proliferation, differentiation and hormonal regulation. *Physiol. Rev.* **66**:855–886
- Nijweide, P.J., Plas, A. van der, Scherft, J.P. 1981. Biochemical and histological studies on various bone cell preparations. *Calcif. Tissue Int.* **33**:529–540
- Petersen, O.H., Maruyama, Y. 1984. Calcium-activated potassium channels and their role in secretion. *Nature (London)* **307**:693–696
- Ypey, D.L., Clapham, D.E. 1984. Development of a delayed outward-rectifying K<sup>+</sup> conductance in cultured mouse peritoneal macrophages. *Proc. Natl. Acad. Sci. USA* **81**:3083–3087
- Ypey, D.L., Ravestloot, J.H., Nijweide, P.J., Buisman, H.P. 1987. Voltage activated ionic channels and conductances in cultured osteoblasts. *Calcif. Tissue Int. (Suppl. 2)*:**41**:78 (abstr.)

Received 15 July 1987; revised 28 October 1987